Magneto-Optical Effect due to Eu^{2+} Ion

Akira YANASE*) and Tadao KASUYA

Department of Physics, Tohoku University, Sendai

(Received November 30, 1970)

The photo absorption and the magneto-optic properties of Eu^{2+} in EuF_2 have been calculated and compared with experiments. Various calculations so far done are not complete because all of them neglected some important interactions to make the calculations performable. Here the amounts of all the important interactions have been checked carefully and the calculations have been performed in various ratios of these parameters. It has been shown from the best fit with the experiments that the multipole-multipole Coulomb interaction and the anisotropic exchange interaction between the $5d$ and $4f$ electrons cancel out each other which leaves nearly isotropic exchange interaction. The absorption structure in such a case has been shown to be similar to that of Freiser's model in which all the $5d$-$4f$ interactions were completely neglected.

§1. Introduction

The divalent europium ion (Eu^{2+}) in EuF_2 and alkaline earth fluorides produce two broad optical absorption bands separated from each other about 2eV. These two bands have been considered to be due to transitions from the $4f^7(^8S)$ ground state of Eu^{2+} to states in the $4f^6 5d$ configuration. The band of longer wave length has an unusual asymmetric shape,[1),2),3)] and a large Faraday rotation is also observed.[4)]

It was assumed by Shen[5)] that the Hund rule is applicable for the optically active excited levels of the $4f^6 5d$ configuration, that is, ^8P_J, in which J runs from 5/2 to 9/2. This implies that the cubic crystal field has no effect because the orbital state is of P-character. However, this is true only when the cubic crystal field is much smaller than the energy separation of the different L terms, which is now due to the multipole Coulomb interaction and the multipole type exchange interaction between $5d$ and $4f^6$ electrons. This is, however, very questionable because the crystal field splitting of $5d$ states, that is, $10Dq$, is usually larger than 1eV, while the energy separation of the different L terms in the octet state is several tenths eV or less.

Recently the other limit of model was proposed by Freiser et al.[2)] Within the first peak corresponding to e_g state, they found seven small peaks which correspond very well to the seven multiplet of $^7F_J(4f^6)$, which is the ground $4f^6$ configuration and J runs from 0 to 6.[2)] Based on these facts, they con-

*) Present address: Ruhr University Bochum, Bochum, West Germany.

sidered that the interactions between $5d$ and $4f$ electrons may be very small and so neglected them completely, and showed that the experiment is fairly well explained. However, there remains the question why the $5d$-$4f$ interaction, particularly the exchange interactions, are negligible, because they are expected to be about 1 eV and thus are at least comparable with the l-s coupling in $4f$ states. In this paper, we examine the values of various interactions and what happens when these interactions are included.

The Hamiltonian is given in §2, the eigen values and the eigen states are given in §3, and the results of numerical calculation are shown and discussed in §4. By using these results, the magneto-optical effects are also discussed in §4.

§2. Hamiltonian

Here we assume that the absorption process is purely of intra-atomic properties. This seems to be a fairly good approximation because the spectra of Eu^{2+} ions in various materials, for example, EuF_2, CaF_2, SrF_2 and BaF_2, are very similar to each other.[1),2)] Then the important interactions are as follows.

$$H=V_{cd}+V_{cf}+\lambda_d \boldsymbol{l}_d \boldsymbol{S}_d+\zeta_f \sum_i \boldsymbol{l}_{fi} \boldsymbol{S}_{fi}+H_{df}+H_{ff}, \tag{1}$$

where, V_{cd} and V_{cf} are the cubic crystal fields for $5d$ and $4f$ electrons respectively and V_{cf} is neglected hereafter because of its smaller effect, λ_d and ζ_f the spin-orbit coupling constants for $5d$ and $4f$ respectively, H_{df} the Coulomb and exchange interactions between $5d$ and $4f$ electrons, and H_{ff} the Coulomb and exchange interaction between $4f$ electrons.

It is natural to put $10Dq=-16000\text{cm}^{-1}$ which corresponds to the separation of two absorption peaks. The following values are obtained from the atomic spectra data for Eu^{3+},[6)]

$$\zeta_f=1415\text{cm}^{-1}, \tag{2}$$

on the basis that the spin-orbit parameter for a $4f$ electron changes very little with the degree of ionization. This value will be supported in the following discussions. The values for λ_d increases gradually from La to Yb[7),8),10),12)] as shown in Fig. 1. From the figure, a reasonable value for Eu^{2+} is concluded to be 1020cm^{-1}. The overall splitting due to the third term of Eq. (1) is estimated to be 2550cm^{-1}. The fourth term in Eq. (1) may be written as

$$\Lambda_f \boldsymbol{L}_f \boldsymbol{S}_f \tag{3}$$

for ${}^7F_J(4f^6)$ configurations in which

$$\Lambda_f=\frac{1}{6}\zeta_f=235.8\text{cm}^{-1}, \tag{4}$$

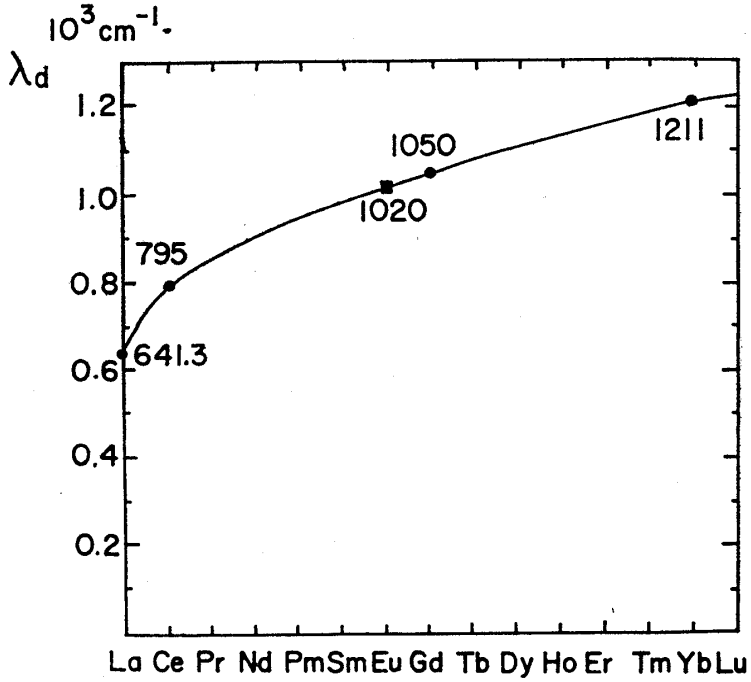

Fig. 1. The spectroscopic data for the spin-orbit interaction of the $5d$-electron of divalent rare earth ions in the configuration of $4f^n5d$; $\lambda_d l_d s_d$. The solid circle marks show the experimental results and the square mark shows the interpolated value for Eu^{2+}. The numbers beside the marks give the precise values in cm^{-1}.

and then overall splitting is $4952.5cm^{-1}$. Note that the nearest excited states $^5D_6(4f^6)$ sit at 2.1eV higher.

The Coulomb and exchange energy between a $5d$ electron and $4f$ electrons with the configuration ^7F are expressed as a function of the total spin S and the total orbital angular momentum L by

$$H_{df}=f_0F_0+f_2F_2+f_4F_4+g_1G_1+g_3G_3+g_5G_5, \qquad (5)$$

Table I. The coefficients of the Slater integrals in the term energy expressions of the $4f^6(^7F)5d$ configuration.

S	L	f_2	f_4	g_1	g_3	g_5
7/2	1	−24	−66	14	−84	−462
	2	−6	99	−21	−84	−462
	3	11	−66	−21	−24	−462
	4	15	22	−21	−84	−462
	5	−10	−3	−21	−84	−252
5/2	1	−24	−66	−7/3	14	77
	2	−6	99	7/2	14	77
	3	11	−66	7/2	4	77
	4	15	22	7/2	14	77
	5	−10	−3	7/2	14	42

Tabe II. The spectroscopic data for the Slater integrals in the d-f interactions of the divalent rare earth ions. The values for Eu^{2+} are obtained by interpolations.

Ions	F_2	F_4	G_1	G_3	G_5
Yb^{2+}	186.8	14.2	193.2	24.62	4.11
Ce^{2+}	175.	21.	296.	40.	5.
Eu^{2+}a	137.2	13.26	184.2	24.31	3.441
b	51.0	13.91	91.84	23.81	7.730

where F_k and G_k are the Slater integrals and the coefficient f_k and g_k were computed by use of the diagonal sum rule. The results are summarized in Table I. Hereafter, we will omit the term of F_0 common to every value of L and S. There are simple relations of

$$f_k(L, S=7/2)=f_k(L, S=5/2) \tag{6}$$

and

$$g_k(L, S=7/2)=-6g_k(L, S=5/2) \tag{7}$$

in these coefficients. The values of the Slater integrals are not known from atomic spectrum data for Eu^{2+} ion. Therefore we should estimate them. Available atomic spectrum data for divalent rare-earth ions are shown in Table II.[8),10)] In Gd^{2+}, the exchange splitting between the states $S=4$ and $S=3$

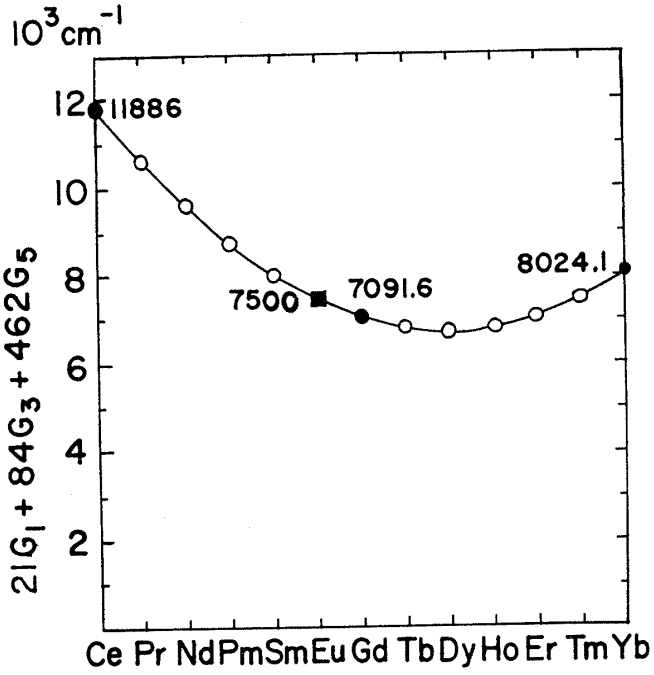

Fig. 2. The values of $21G_1+84G_3+462G_5$ are shown, which gives isotropic exchange interaction between $5d$ and $4f^n$ electrons in divalent rare earth ions. The black circles show the spectroscopic data and the square and the white circles show the interpolated values for Eu^{2+} and the other ions respectively. The numbers beside the marks give the precise values in cm^{-1}.

in $5d4f^7$ configuration is given in the spectroscopic data[7] which gives the value for $21G_1+84G_3+462G_5$. As shown in Fig. 2, a reasonable value for Eu^{2+} is given as 7500 cm^{-1}. The relative ratios between F_k and G_k are estimated by linear interpolation between Ce^{2+} and Yb^{2+} and final results are shown as the third row in Table II. In Table III, the term energies which were computed

Table III. The term energies for the free Eu^{2+} ion in the configuration of $4f^6(^7F)5d$ are shown. These values are calculated from the values of the third row in Table II, and the unit is cm^{-1}.

S	L	Coulomb energy (F_2, F_4)	Exchange energy (G_1, G_3, G_5)	Total
7/2	1	−4167.96	−1052.98	−5220.94
	2	489.54	−7499.98	−7010.44
	3	634.04	−6041.38	−5407.44
	4	2349.72	−7499.98	−5150.26
	5	−1411.78	−6777.37	−8189.15
5/2	1	−4167.96	175.50	−3992.46
	2	489.54	1250.00	1739.54
	3	634.04	1006.90	1640.94
	4	2349.72	1250.00	3599.72
	5	−1411.78	1129.56	−282.22

using these values are shown as an example. Note that differences between the term energies for different L in $S=7/2$ become smaller by a partial cancellation between the Coulomb (F_k) and the exchange (G_k) energies. This cancellation becomes complete, if we choose the parameters as follows,

$$F_2/G_1;\ F_4/G_1;\ G_2/G_1;\ G_3/G_1=5/9;\ 5/33;\ 7/27;\ 25/297. \qquad (8)$$

The values given in the fourth row of Table II were calculated by using these ratios. In this particular ratio, the d-f interaction is given simply by the isotropic exchange type, $2I\mathbf{S}_d\mathbf{S}_f$, the same as the case of Gd^{2+} in the octet state. The actual calculation for the d-f interaction is very difficult because of strong shielding effect of $5s$ and $5p$ states which situate in between $4f$ and $5d$ states. The exchange type interaction may not be affected very much by this shielding effect but the Coulomb type may be affected very strongly. In such a situation the isotropic exchange type interaction may be a good approximation for the $5d$-$4f$ interaction. It is one of the main purposes of this paper to check this point.

§3. Eigen values, eigen states and spectral intensity

The Hamiltonian (1) is expressed in a basis system of

$$|(J_FJ_d)J,\Gamma\alpha\nu\rangle=\sum_{J_Z}A^{\alpha}(JJ_Z,\Gamma\nu)\,|(S_FL_F)J_F,(S_dl_d)J_d;\ JJ_Z\rangle, \qquad (9)$$

where A's are symmetrized coefficients, Γ indicates the irreducible representation of the cubic group, ν is a number of basis functions in the irreducible representation, and α is an extra suffix to distinguish the irreducible representation of the same types with the same J value. There are 82 irreducible representations of type U', 40 of type E' and 41 of type E''. The third and fourth terms in Eq. (1) are diagonal in this representation and are given respectively by

$$\frac{1}{2}\lambda_d\left[J_d(J_d+1)-\frac{1}{2}\cdot\frac{3}{2}-2\cdot 3\right] \tag{10}$$

and

$$\frac{1}{2}\Lambda_F[J_F(J_F+1)-3\cdot 4-3\cdot 4]. \tag{11}$$

The fifth term is diagonal as shown in Eq. (5) in a basis system of

$$|(S_FS_d)S,(L_FL_d)L;\,J\,J_Z\rangle, \tag{12}$$

which can be transformed to Eq. (9) by using the $9j$ symbol as follows,[11]

$$\begin{aligned}&|(S_FL_F)J_F,(S_dL_d)J_d;\,J\,J_Z\rangle\\&\quad=\sum_{S,L}|(S_FS_d)S,(L_FL_d)L;\,J\,J_Z\rangle\\&\quad\times\sqrt{(2J_F+1)(2J_d+1)(2S+1)(2L+1)}\begin{Bmatrix}3 & 1/2 & S\\ 3 & 2 & L\\ J_F & J_d & J\end{Bmatrix}.\end{aligned} \tag{13}$$

In order to get the expression for the left-hand side of Eq. (13), the following transformation is necessary:[11]

$$\begin{aligned}&|(S_FL_F)J_F,(S_dL_d)J_d;\,J\,J_Z\rangle\\&\quad=\sum_{J_{FZ}J_{dZ}}|(S_FL_F)J_FJ_{FZ}\rangle|(S_dL_d)J_dJ_{dZ}\rangle\\&\qquad\times\langle J_FJ_dJ_{FZ}J_{dZ}|JJ_Z\rangle\end{aligned} \tag{14}$$

and

$$\begin{aligned}&|(S_dL_d)J_dJ_{dZ}\rangle\\&\quad=\sum_{S_{dZ}L_{dZ}}|S_dS_{dZ}\rangle|L_dL_{dZ}\rangle\langle S_dL_dS_{dZ}L_{dZ}|J_dJ_{dz}\rangle.\end{aligned} \tag{15}$$

In the above equations, the Clebsch-Gordan coefficient, $\langle j_1j_2m_1m_2|Jm\rangle$, is used. Moreover, the following relations are well known,

$$V_{cd}|t_{2g}^{\mu}\rangle=-4Dq|t_{2J}^{\mu}\rangle \tag{16}$$

and

$$V_{cd}|e_g^{\mu}\rangle=6Dq|eq_g^{\mu}\rangle, \tag{17}$$

where

$$|e_g^1\rangle=\frac{1}{\sqrt{2}}(|L_d 2\rangle+|L_d -2\rangle), \tag{18}$$

$$|e_g^2\rangle=|L_d 0\rangle \tag{19}$$

and

$$|t_{2g}^1\rangle=|L_d -1\rangle, \tag{20}$$

$$|t_{2g}^0\rangle=\frac{1}{\sqrt{2}}(|L_d 2\rangle-|L_d -2\rangle), \tag{21}$$

$$|t_{2g}^{-1}\rangle=-|L_d 1\rangle. \tag{22}$$

By using these equations, we can calculate the matrix elements of the Hamiltonian (1) in the basis system of Eq. (9), and diagonalize them to obtain the eigen values, E_β^Γ, and the eigen states, $|\psi_e, \Gamma\beta\nu\rangle$.

$$H|\psi_e, \Gamma\beta\nu\rangle=E_\beta^\Gamma|\psi_e, \Gamma\beta\nu\rangle, \tag{23}$$

$$|\psi_e, \Gamma\beta\nu\rangle=\sum_{JJ_FJ_d\alpha} B_\beta^\Gamma(J\,J_F J_d\alpha)\,|\,(J_F J_d)J, \Gamma\alpha\nu\rangle. \tag{24}$$

In the next, the matrix element of the electric dipole transition is calculated. At first, the following matrix element is obtained.

$$\langle {}^8S(4f^7)S_{gz}|\sum_i x_{i\eta}|\,(S_F S_d)S, (L_F L_d)L;\, J\,J_z\rangle$$
$$=-|e|\sqrt{\frac{5}{3}}(d\|r\|f)\delta_{S,7/2}\delta_{L,1}\left\langle\frac{7}{2}1S_{gz}\eta\,|\,J\,J_z\right\rangle, \tag{25}$$

where e is the electronic charge, $x_{i\eta}$ the irreducible tensor component of the electric dipole operator for i-th electron and $(d\|r\|f)$ the $5d$-$4f$ radial integral,

$$(d\|r\|f)=\int_0^\infty dr\, r\, R_{4f}(r)R_{5d}(r) \tag{26}$$

and $R(r)/r$ is the radial part of the one-electron orbital function. Then the matrix element for optical absorption is given as follows,

$$\langle {}^8S(4f^7)S_{gz}|\sum_i x_{i\eta}|\psi_e, \Gamma\beta\nu\rangle$$
$$=-|e|\,(d\|r\|f)P_{\beta\nu}^\Gamma(S_{gz}\eta), \tag{27}$$

where

$$P_{\beta\nu}^\Gamma(S_{gz}\eta)=\sqrt{\frac{5}{3}}\sum_{J\alpha}\overline{B}_\beta^\Gamma(J\alpha)Q_\nu^\Gamma(J\alpha, S_{gz}\eta) \tag{28}$$

and

$$B_{\beta}^{\Gamma}(J\alpha)=\sum_{J_F J_d} B_{\beta}^{\Gamma}(J\,J_F J_d\alpha) \times\sqrt{24(2J_F+1)(2J_d+1)}\begin{Bmatrix}3 & 1/2 & 7/2\\ 3 & 2 & 1\\ J_F & J_d & J\end{Bmatrix} \tag{29}$$

and

$$Q_{\nu}^{\Gamma}(J\alpha, S_{gz}\eta)=A^{\alpha}(JS_{gz}+\eta, \Gamma\nu)\left\langle\frac{7}{2}1\, S_{gz}\eta\,|\,JS_{gz}+\eta\right\rangle. \tag{30}$$

There are the following orthogonality relations,

$$\sum_{S_{gz}\eta} Q_{\nu}^{\Gamma}(J\alpha, S_{gz}\eta)Q_{\nu'}^{\Gamma'}(J'\alpha', S_{gz}\eta)=\delta_{\Gamma\Gamma'}\delta_{\nu\nu'}\delta_{JJ'}\delta_{\alpha\alpha'} \tag{31}$$

and

$$\sum_{S_{gz}\nu} Q_{\nu}^{\Gamma}(J\alpha, S_{gz}\eta)Q_{\nu}^{\Gamma}(J'\alpha', S_{gz}\eta)=\frac{n_{\Gamma}}{3}\delta_{\alpha\alpha'}\delta_{JJ'}, \tag{32}$$

(not depend on η)

where n_{Γ} indicates the degeneracy of the irreducible representation Γ. Therefore, the following relation is obtained:

$$\sum_{S_{gz}\nu}|P_{\beta\nu}^{\Gamma}(S_{gz}\eta)|^2=\frac{5}{9}n_{\Gamma}\sum_{J\alpha}|\bar{B}_{\beta}^{\Gamma}(J\alpha)|^2. \tag{33}$$

(not depend on η)

This implies that the dichroism occurs only when the probability $p(S_{gz})$, for the ground state to be in $|^8S(4f^7)S_{gz}\rangle$, depends on S_{gz}.

The optical absorption coefficient is given by

$$\alpha_{\eta}(E)=CEf_{\eta}(E), \tag{34}$$

where

$$C=\frac{4\pi^2Ne^2}{hc}(d/\!/r/\!/f)^2\left[\frac{(n_0^2+2)^2}{9n_0}\right] \tag{35}$$

and

$$f_{\eta}(E)=\sum_{S_{gz}\Gamma\nu\beta} p(S_{gz})\,|P_{\beta\nu}^{\Gamma}(S_{gz}\eta)|^2 G(E_{\beta}^{\Gamma}-E_g-E). \tag{36}$$

Where n_0 is the index of refraction, N the number density of Eu^{2+} ion, E_g the energy of the ground state ^8S and $G(E)$ is the structural function due to the electron-phonon interaction, and is assumed in the following discussion, for simplicity, as the Gaussian type as follows,

$$G(E)=\frac{1}{\sqrt{2\pi}\,\Delta}\exp[-(1/2)(E/\Delta)^2], \tag{37}$$

where the value for Δ is taken as $300\,\mathrm{cm}^{-1}$ from the experimental results at high temperature.

The contribution from electric susceptibilities to the Faraday rotation per

unit length is given by the Kramers-Kronig relation as follows,[12]

$$\theta(E)=\frac{C}{4\pi}\Theta(E), \tag{38}$$

$$\Theta(E)=E^2\int dE'\frac{f_+(E')-f_-(E')}{E'^2-E^2}. \tag{39}$$

§4. Numerical results

At first, several limiting cases are discussed in order to show what happens when various interactions are included. When F_k, G_k and λ_d tend to zero, the eigen values and the eigen states are given as follows,

$$H|(S_FL_F)J_FJ_{FZ}\rangle|S_dS_{dz}\rangle|L_d\Gamma\nu\rangle = (E_{J_F}+E_\Gamma)|J_FJ_{FZ}\rangle|S_dS_{dz}\rangle|L_d\Gamma\nu\rangle, \tag{40}$$

where

$$E_{J_F}=\frac{1}{2}A_F(J_F(J_F+1)-24), \tag{41}$$

$$E_\Gamma=\begin{cases}6Dq, & (\Gamma=e_g)\\ -4Dq, & (\Gamma=t_{2g})\end{cases} \tag{42}$$

$$J_F=0,1,2,\cdots,6 \tag{43}$$

and $|L_d\Gamma\nu\rangle$ is given in (18)$\sim$(22). This is the model of Freiser et al.

The l-s coupling within $5d$ makes $^2t_{2g}$ split into E'' and U'. On the other hand, it has no matrix-elements within ^2e_g. However there are matrix elements between U' in $^2t_{2g}$ and U' of ^2e_g given by

$$(U'(^2t_{2g})\nu|\lambda_d\boldsymbol{l}_d\boldsymbol{S}_d|U'(^2e_g)\nu'\rangle=-\frac{\sqrt{6}}{2}\lambda_d\delta_{\nu\nu'}. \tag{44}$$

Hence the second order perturbation gives the energy shift for ^2e_g,

$$-\frac{6}{4}\cdot\frac{\lambda_d^2}{10Dq}=98\text{cm}^{-1} \tag{45}$$

for the values given in §2. As shown in Fig. 3, the effects of the λ_d term on the spectral intensity are detectable even in the e_g band.

The Coulomb and exchange energy mainly give the exchange splitting as shown in Table III. Then the following limiting cases are examined.

$$\lambda_d=0 \tag{46}$$

and

$$H_{df}=-I\boldsymbol{S}_d\boldsymbol{S}_f-A_I, \tag{47}$$

where the following values of I and A_I are used.

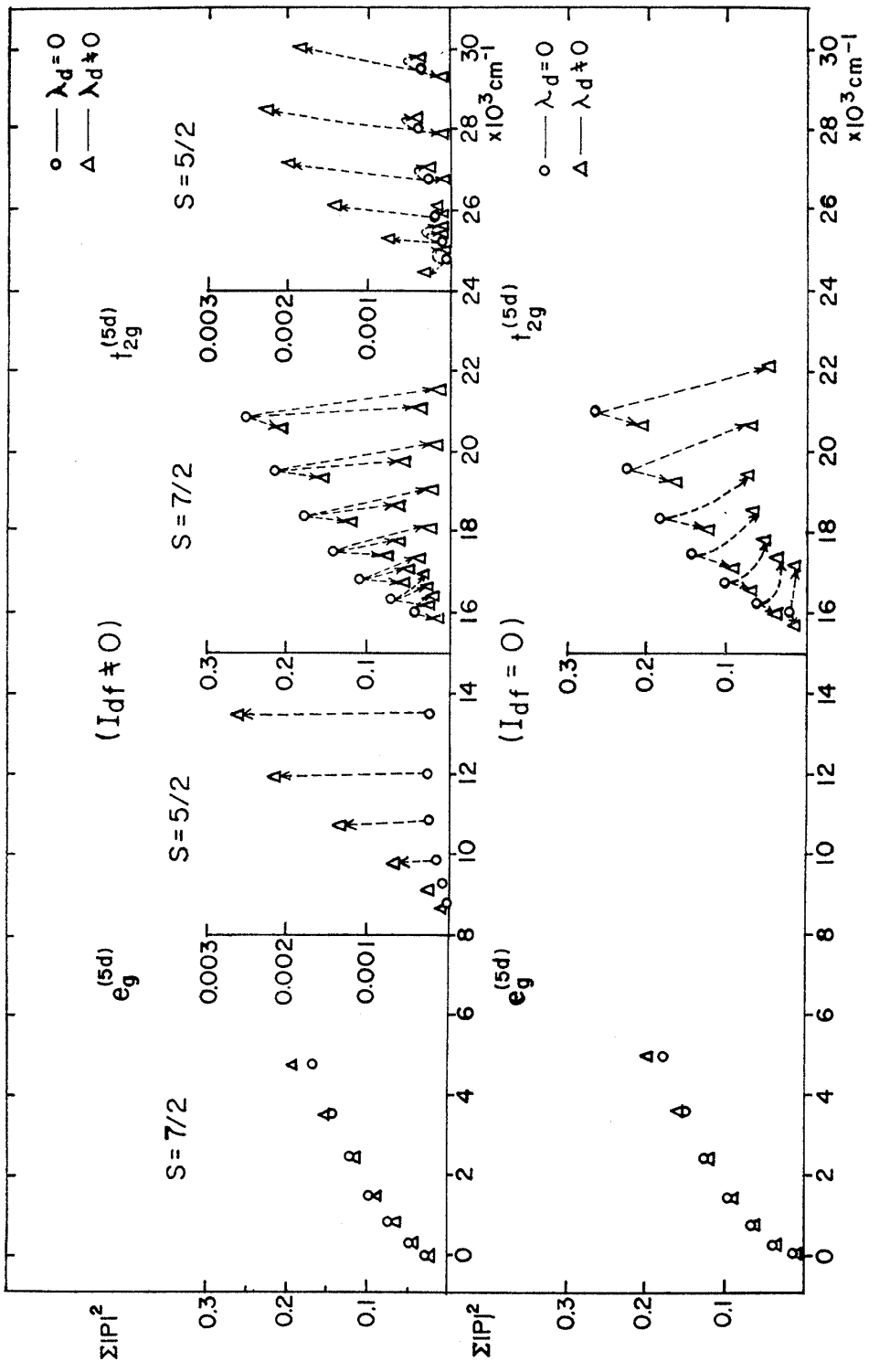

Fig. 3. Absorption intensity for each level is shown in the four kinds of limiting cases.

$$I=2500\text{cm}^{-1}, \tag{48}$$

$$A_I=5000\text{cm}^{-1}. \tag{49}$$

Since the I-term is much larger than the Λ_F-term, the eigen values and the eigen states are given approximately as follows,

$$H|(S_dS_F)SL_F;\ J_AJ_{AZ}\rangle|L_{d\Gamma},\nu\rangle = (E(J_A,S)+E_\Gamma)|S,J_AJ_{AZ}\rangle|L_{d\Gamma},\nu\rangle, \tag{50}$$

where

$$S=7/2,5/2, \tag{51}$$

$$J_A=1/2,3/2,\cdots,13/2, \quad (S=7/2) \tag{52}$$

$$J_A=1/2,3/2,\cdots,11/2 \quad (S=5/2) \tag{53}$$

and

$$E(J_A,S=7/2)=-A_I-\frac{3}{2}I+\frac{3}{7}\Lambda_F(J_A(J_A+1)-111/4), \tag{54}$$

$$E(J_A,S=5/2)=-A_I+2I+\frac{4}{7}\Lambda_F(J_A(J_A+1)-83/4). \tag{55}$$

The Λ_F-term has the following non-diagonal matrix elements,

$$\langle S=7/2,J_AJ_{AZ}|\Lambda_F\boldsymbol{S}_F\boldsymbol{L}_F|S=5/2,J'_AJ'_{AZ}\rangle = \frac{\Lambda_F}{28}(2J_A+1)\sqrt{(J_A+15/2)(13/2-J_A)}\,\delta_{J_AJ'_A}\delta_{J_AZJ'_{AZ}}, \tag{56}$$

which becomes maximum 1.75 Λ_F at $J_A=9/2$ and gives the second order shift of

$$\frac{(1.75\Lambda_F)^2}{(7/2)I}\simeq 20\text{cm}^{-1}. \tag{57}$$

The non-diagonal elements of Eq. (56) are so small that the absorption intensity for spin-orbit allowed transition is very small, and is about 1/1000 of spin allowed transition as shown in Fig. 3.

In Fig. 3, the results for the case of $\lambda_d\neq 0$ are also shown. Within t_{2g} configuration, $\lambda_d\boldsymbol{l}_d\boldsymbol{S}_d$ is rewritten as

$$\lambda_t\boldsymbol{l}_t\boldsymbol{S}_t \tag{58}$$

in which $\lambda_t=\lambda_d$ and the conversion of Eqs. (20)$\sim$(22) should be done. When λ_d is introduced, each J_A level splits into three J_T levels of

$$J_T=J_A-1,J_A,J_A+1 \tag{59}$$

and by the inter J_A matrix element, the levels of different J_A origin but of the same J_T mix each other. Moreover, the non-diagonal element between e_g

and t_{2g} states introduces small splitting in $|J_T, J_{TZ}\rangle$ of within $20cm^{-1}$. The effect of λ_d-term on e_g states is only due to these non-diagonal matrix elements, which give a small splitting of within also $20cm^{-1}$, intensity modifications and the second order shifts. In this case, the intensity of the spin-orbit allowed transition of e_g states become 1/100 of the spin allowed transition. This is mainly due to the mixing with t_{2g} states.

In Fig. 4, the intensities for the case of $S_{gz}=7/2$ are shown for three polarizations of light. The differences between + and − polarization give the

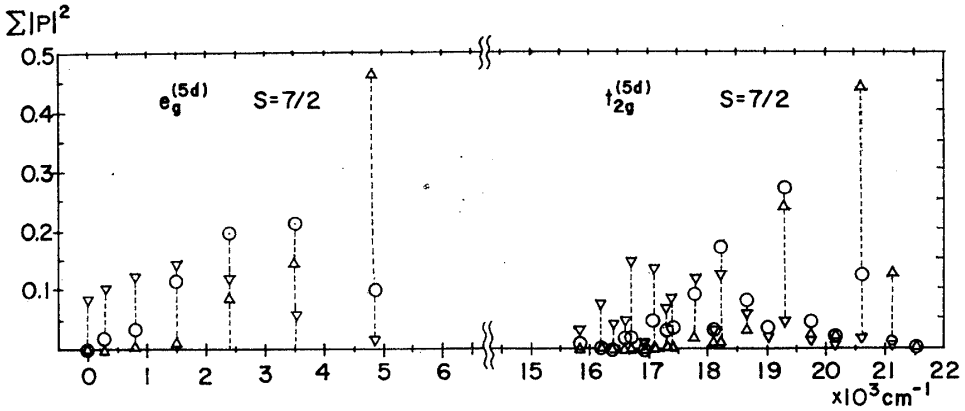

Fig. 4. Circular and linear dichroism for the simplified Hamiltonian $H=V_{cd}+A_F\boldsymbol{S}_F\boldsymbol{L}_F+\lambda_d\boldsymbol{S}_d\boldsymbol{L}_d-I\boldsymbol{S}_d\boldsymbol{S}_F$ are shown, in which the ground state $4f^7$ ($^8S_{7/2}$) is assumed to be fully polarized. The triangle marks indicate the absorption intensity for the light with plus polarization, the reverse triangle marks for minus polarization and the circle marks for parallel polarization.

circular dichroism, and the differences between 0 polarization and the mean values of + and − polarization give the linear dichroism.

The Coulomb and exchange interaction between $5d$ and $4f$ electrons which was shown in Eq. (5) are expressed more generally, containing the configuration mixing or the shieldings due to $5s^2$ and $5p^6$ electrons, by using the seven parameters of A_K and B_K.

$$H_{df}=\sum_{K=2,4}A_KS_K-\frac{1}{6}[3+2(\boldsymbol{S}_d\boldsymbol{S}_F)]\sum_{K=0}^{4}B_KS_K, \tag{60}$$

where S_K is the scalar product of the two irreducible tensor operators of $T_q^{(K)}$ and $U_q^{(K)}$. The former is for the $4f$ electrons and the latter is for the $5d$-electron. Namely

$$S_K\equiv(T^{(K)}\cdot U^{(K)})=\sum_q(-)^qT_q^{(K)}U_{-q}^{(K)} \tag{61}$$

and

$$\langle L_FM_F|\,T_q^{(K)}\,|L_FM_F'\rangle=\frac{(-)^{3-M_F'}}{\sqrt{(2K+1)}}\langle 3\,3\,M_F-M_F'|Kq\rangle, \tag{62}$$

$$\langle L_d M_d | U_q^{(K)} | L_d M_d' \rangle = \frac{(-)^{2-M_D'}}{\sqrt{(2K+1)}} \langle 2\,2\,M_d - M_d' | Kq \rangle. \tag{63}$$

Moreover

$$\langle (L_F L_d) L, L_Z | S_K | (L_F L_d) L', L_Z' \rangle = \delta_{L,L'} \delta_{L_Z,L'_Z} (-)^{L+1} \begin{Bmatrix} 3 & K & 3 \\ 2 & L & 2 \end{Bmatrix}. \tag{64}$$

Table IV. The matrix elements for the scalar product S_K.

L \ K	0	1	2	3	4
1	1	−8	24	−6	66
2	1	−6	6	3	−99
3	1	−3	−11	4	66
4	1	1	−15	−4	−22
5	1	6	10	1	3
Common factor t_K	$\sqrt{1/35}$	$\sqrt{1/2520}$	$\sqrt{1/29400}$	$\sqrt{1/2940}$	$\sqrt{1/873180}$

The values of Eq. (64) are given in Table IV. If we neglect the configuration mixing, the values for the coefficients A_K and B_K are given by F_K and G_K as follows:

$$A_2 = -\frac{1}{t_2}(F_2), \tag{65}$$

$$A_4 = -\frac{1}{t_4}(F_4), \tag{66}$$

$$B_0 = \frac{6}{7t_0}(21G_1 + 84G_3 + 462G_5), \tag{67}$$

$$B_1 = \frac{1}{2t_1}(2G_1 + 3G_3 - 33G_5), \tag{68}$$

$$B_2 = \frac{1}{14t_2}(-6G_1 + 11G_3 - 55G_5), \tag{69}$$

$$B_3 = \frac{1}{2t_3}(3G_1 - 8G_3 - 11G_5), \tag{70}$$

$$B_4 = \frac{1}{14t_4}(-G_1 - 4G_3 - G_5), \tag{71}$$

in which t_K are given in Table IV. Using these expressions, the Coulomb and exchange energies for $S=7/2$ states are given as follows:

$$E_Q(L, S=7/2) = \sum_{K=0}^{4} C_K (S_K/t_K), \tag{72}$$

where

$$C_0 = -\frac{6}{7}(21G_1 + 84G_3 + 462G_5), \tag{73}$$

$$C_1=-\frac{1}{2}(2G_1+3G_3-33G_5), \tag{74}$$

$$C_2=-\frac{1}{14}(14F_2-6G_1+11G_3-55G_5), \tag{75}$$

$$C_3=-\frac{1}{2}(3G_1-8G_3-11G_5), \tag{76}$$

$$C_4=-\frac{1}{14}(14F_4-G_1-4G_3-G_5). \tag{77}$$

Matrix elements of $T_q^{(K)}$ are given in basis system of $|(S_dS_F)SL_F; J_AJ_{AZ}\rangle$ as follows,

$$\begin{aligned}&\langle(S_dS_F)SL_F; J_AJ_{AZ}|\, T_q^{(K)}\,|(S_dS_F)S'L_F; J'_AJ'_{AZ}\rangle\\&=\frac{\delta_{SS'}}{\sqrt{2K+1}}(-)^{J_A+J'_A+S+K+3-J'_{AZ}}\sqrt{(2J_A+1)(2J'_A+1)}\begin{Bmatrix}3 & K & 3\\ J'_A & S & J_A\end{Bmatrix}\\&\times\langle J_AJ'_AJ_{AZ}-J'_{AZ}|Kq\rangle.\end{aligned} \tag{78}$$

In the e_g states, among the $U_q^{(K)}$, only $U_0^{(0)}$, $U_0^{(2)}$, $U_{\pm2}^{(2)}$, $U_{\pm2}^{(3)}$, $U_0^{(4)}$, $U_{\pm2}^{(4)}$ and $U_{\pm4}^{(4)}$ have non-zero matrix element as follows:

$$\langle e_g^1|\,U_0^{(0)}\,|e_g^1\rangle=\frac{1}{\sqrt{5}}, \tag{79}$$

$$\langle e_g^2|\,U_0^{(0)}\,|e_g^2\rangle=\frac{1}{\sqrt{5}}, \tag{80}$$

$$\langle e_g^1|\,U_0^{(2)}\,|e_g^1\rangle=\sqrt{\frac{2}{35}}, \tag{81}$$

$$\langle e_g^2|\,U_0^{(2)}\,|e_g^2\rangle=-\sqrt{\frac{2}{35}}, \tag{82}$$

$$\langle e_g^1|\,U_{\pm2}^{(2)}\,|e_g^2\rangle=\sqrt{\frac{1}{35}}, \tag{83}$$

$$\langle e_g^1|\,U_{\pm2}^{(3)}\,|e_g^2\rangle=\pm\frac{1}{\sqrt{28}}, \tag{84}$$

$$\langle e_g^1|\,U_0^{(4)}\,|e_g^1\rangle=\frac{1}{\sqrt{630}}, \tag{85}$$

$$\langle e_g^2|\,U_0^{(4)}\,|e_g^2\rangle=\sqrt{\frac{2}{35}}, \tag{86}$$

$$\langle e_g^2|\,U_{\pm2}^{(4)}\,|e_g^1\rangle=\sqrt{\frac{1}{84}}, \tag{87}$$

$$\langle e_g^1|\,U_{\pm4}^{(4)}\,|e_g^1\rangle=\sqrt{\frac{1}{36}}, \tag{88}$$

$$\langle e_g^2 | U_{\pm 4}^{(4)} | e_g^2 \rangle = 0. \tag{89}$$

We have caluculated the spectral intensity using the various parameters of the Coulomb and the exchange interactions, and the results are shown in Figs. 5~7. The Fig. 6(K) corresponds to the case of $\lambda_d \neq 0$, $I \neq 0$ in Fig. 3, and the figures (D) in Figs. 5~7 are the results of the calculations by using the values of the fourth row in Table II. In the spin allowed transitions, that is, the transitions to the states of $S=7/2$, the case (K) and (D) give almost the same figures to each other. This implies that the energy splittings in the states of $S=5/2$ have very small effects on the spin allowed transitions.

The series from (A) to (D) shows the effects of the energy splittings within the states with $S=7/2$, that is the effects of the S_1, S_2, S_3 and S_4 terms in Eq. (72). The figures (A) are the results of the calculations using the values in the third row in Table II. Moreover, in (C), the mean values of (A) and (D) are used, and the mean values of (A) and (C) are used in

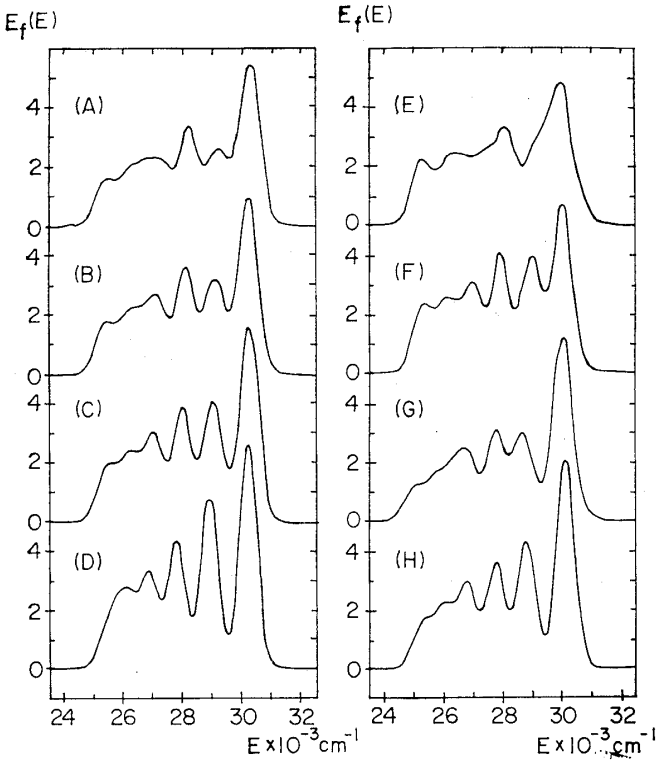

Fig. 5. The absorption curves for the spin allowed ($S=7/2$) transitions into the e_g band are shown. The anisotropic parts of the Coulomb and the exchange interactions are shown in Table V.

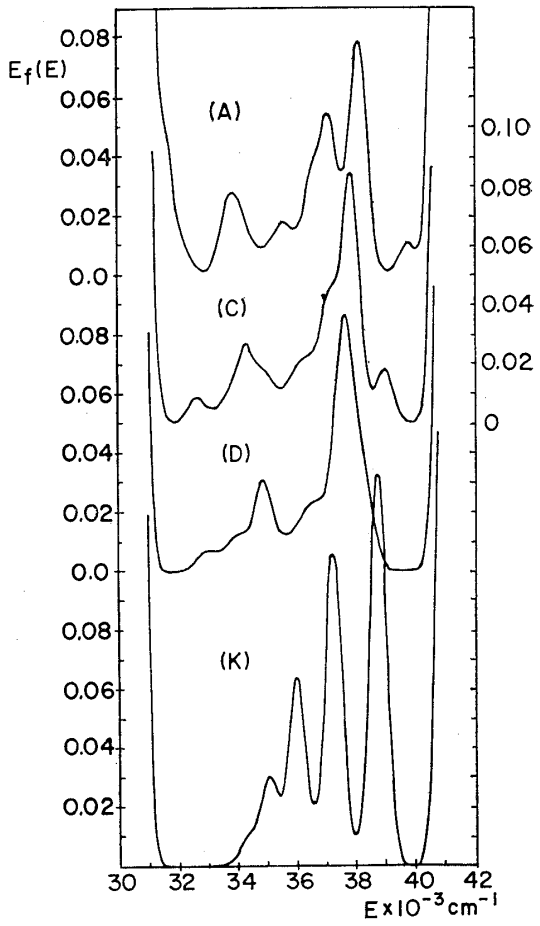

Fig. 6. The absorption curves for the spin-orbit allowed ($S=5/2$) transitions into the e_g band are shown.

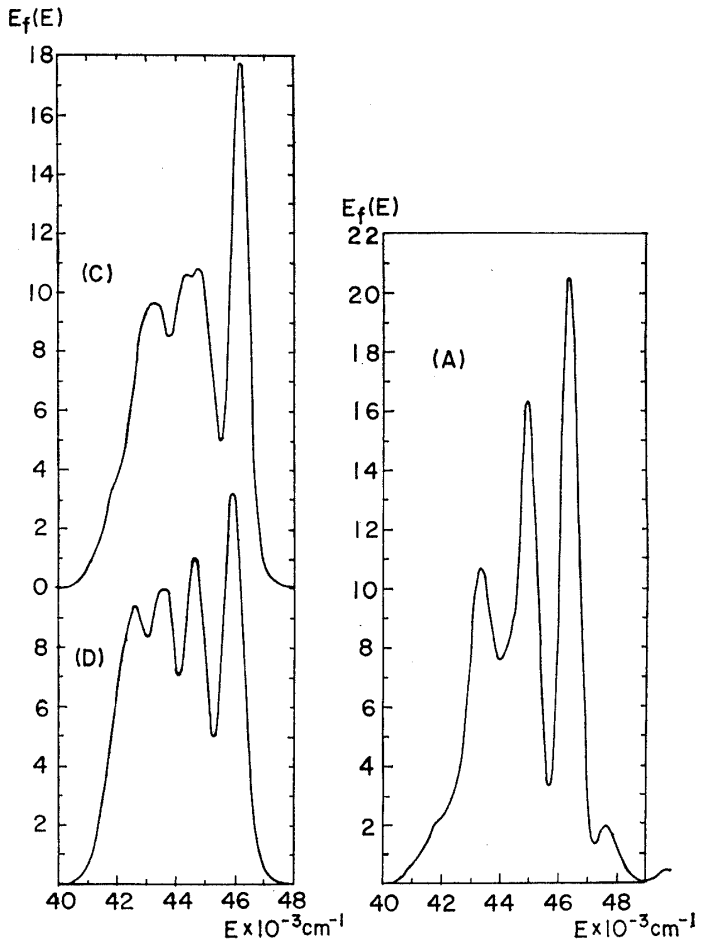

Fig. 7. The absorption curves for the spin allowed ($S=7/2$) transitions into the t_{2g} band are shown.

Table V. The values for the anisotropic parts of the Coulomb and the exchange interactions in the states with $S=7/2$.

The cases	C_1	C_2	C_3	C_4
A	−163.9	−63.8	−160.1	7.1
B	−122.9	−47.9	−120.1	5.3
C	−81.9	−31.9	−80.1	3.5
D	0.	0.	0.	0.
E	−151.7	−100.2	−157.7	6.5
F	−75.9	−50.1	−78.8	3.2
G	−172.6	−37.8	−161.8	7.5
H	−86.3	−18.9	−80.9	3.8

(B). Therefore the absolute values of C_K decreases from (A) to (D) as shown in Table V. The peaks become, of course, more sharp with decreasing values of C_K. However the peak of the lowest energy is more sharp in (C) than in (D). The peak of the lowest energy in (C) is composed of two

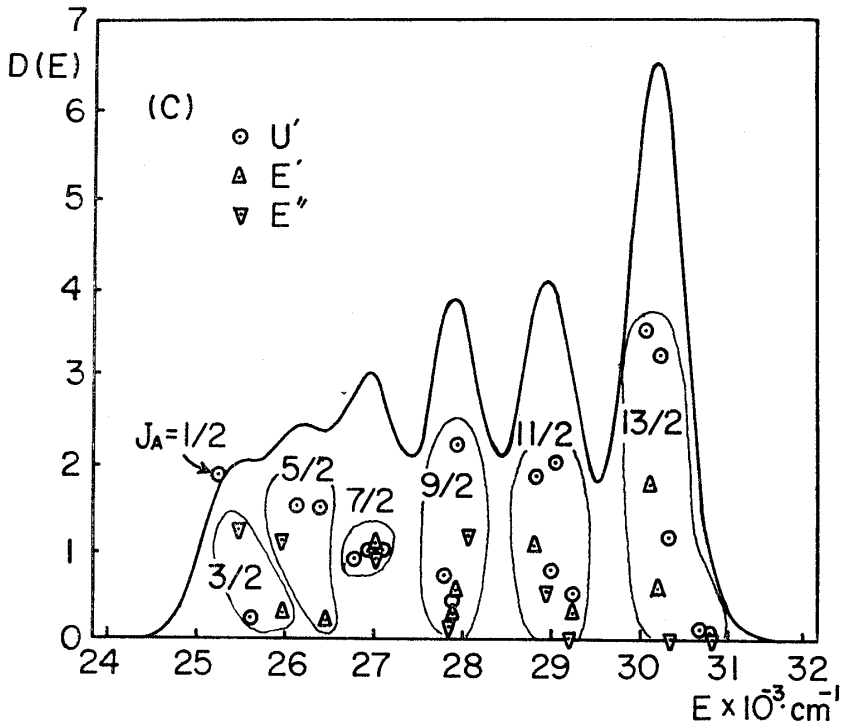

Fig. 8. The splittings of various J_A states into U', E' and E'' due to the anisotropic parts of the Coulomb and the exchange interactions and the effect on the absorption curve. The values of parameters for the case C are shown in Table V.

kinds of states, U' of the states $J_A=1/2$ and E'' of $J_A=3/2$ as shown in Fig. 8. The level splitting of $J_A=3/2$ states due to C_2 and C_3 terms in Eq. (72) overcomes the line broadenings due to the electron phonon interaction. In the case of (D) on the other hand, the peak of $J_A=3/2$ is overlapped with the peak of $J_A=5/2$ by the broadening due to the electron phonon interaction, which is assumed to be 300cm^{-1}. In the spectral data for Ce^{2+} and Yb^{2+}, the ratios between F_K and G_K are quite different from each other as shown in Table II. Therefore we have also calculated the spectral intensity using the ratio of F_K and G_K of Yb^{2+} and Ce^{2+}. The cases of (E) and (G) correspond to the cases of Yb^{2+} and Ce^{2+} respectively. Moreover, in the cases of (F) and (H) the mean values between (D) and (E), and (D) and (G) are used respectively. Among the many figures in Fig. 5, (C) and (H) are in good agreement with the experimental results. Note that (C) and (H) are better than (D) in the lower energy region. The values of C_K for the various cases are shown in Table V. From this table and Fig. 5, it can be concluded that the values of C_2 should be about $-20\sim-30$ cm^{-1}, and the overall splitting due to S_2, S_3 and S_4 should be less than about 2000cm^{-1} in order to give the peaks observed in the absorption spectrum of Eu^{2+} in EuF_2. However we cannot determine more precise values for F_K and G_K, or A_K and B_K from the experimental results.

The data which can be used in the further discussion was given in the Zeeman effect for the lowest U' level observed by Kisliuk et al.[3] The magnetic splitting of U' levels is, in general, not isotropic and a fomula for its angular dependence is given by

$$(W/\mu_B H)^2=\frac{1}{4}[\xi_1^2+\xi_2^2]\pm\frac{\xi_1}{2}\sqrt{\xi_2^2+\frac{3}{4}[\xi_1^2-4\xi_2^2](l^2m^2+m^2n^2+n^2l^2)}, \quad (90)$$

where W is the energy shift, μ_B the Bohr magneton, H the magnetic field intensity, ξ_1 and ξ_2 are parameters characterizing the splitting, and l, m and n direction cosines of the field direction. If the direction of the field is $\langle 100\rangle$,

$$(W/\mu_B H)_k=\frac{1}{2}(\xi_1+\xi_2), \quad (91)$$

$$(W/\mu_B H)_\lambda=\frac{1}{2}(\xi_1-\xi_2), \quad (92)$$

$$(W/\mu_B H)_\mu=\frac{1}{2}(-\xi_1+\xi_2), \quad (93)$$

$$(W/\mu_B H)_\nu=\frac{1}{2}(-\xi_1-\xi_2), \quad (94)$$

in which k, λ, μ and ν imply the symmetries of the wave functions and $|U'_k\rangle$, $|U'_\lambda\rangle$, $|U'_\mu\rangle$ and $|U'_\nu\rangle$ have the symmetries of $|J=3/2,\ J_z=3/2\rangle$, $|3/2,\ 1/2\rangle$, $|3/2,\ -1/2\rangle$ and $|3/2,\ -3/2\rangle$, respectively. The following value for the lowest U' state was determined experimentally,

$$\xi_1=0.7 \quad \text{and} \quad \xi_2=3.5. \quad (95)$$

In the states of $|U';\ S=7/2,\ J_A=1/2,\ e_g\rangle$, which are considered approximately as the wave functions for the lowest state, the four states having the symmetry of k, λ, μ and ν are expressed as follows:

$$U_k=|-1/2\rangle|e_g^1\rangle, \quad (96)$$

$$U_\lambda=-|1/2\rangle|e_g^2\rangle, \quad (97)$$

$$U_\mu=|-1/2\rangle|e_g^2\rangle, \quad (98)$$

$$U_\nu=-|1/2\rangle|e_g^1\rangle \quad (99)$$

and the g-factor for the state $|(S=7/2, L_F)J_A=1/2\rangle$ is given by

$$\frac{3J_A(J_A+1)+S(S+1)-L_F(L_F+1)}{2J_A(J_A+1)}=4. \quad (100)$$

Therefore the Zeeman splitting for the states of $J_A=1/2$ is given as follows:

$$(W/\mu_B H)_k=+2,\quad (W/\mu_B H)_\lambda=-2,\quad (W/\mu_B H)_\mu=+2$$

and $$(W/\mu_B H)_\nu=-2,$$

and then the values of $\xi_2=4$ and $\xi_1=0$ are given.

When the S_K terms with none zero value of K are introduced, the state of $J_A=1/2$ is mixed with the states which have higher J_A values and then the Zeeman splitting is modified as follows,

$$(W/\mu_B H)_k=2+\sum_{J_A\neq 1/2}\sum_{K\neq 0}\frac{C_K\langle U'_k 1/2|2S_z+L_z|U'_k J_A\rangle\langle U'_k J_A|S_K|U'_k 1/2\rangle}{E(J_A)-E(1/2)}$$
$$+(\text{higher order terms}), \tag{101}$$

where $|U'_k J_A\rangle$ is an abbreviated expression for $|U'_k; S=7/2, J_A, e_g\rangle$ and, for example,

$$|U'_k 3/2\rangle=\frac{1}{\sqrt{2}}(|3/2\rangle|e_g^2\rangle+|-1/2\rangle|e_g^1\rangle), \tag{102}$$

$$|U'_\lambda 3/2\rangle=\frac{1}{\sqrt{2}}(-|1/2\rangle|e_g^2\rangle+|-3/2\rangle|e_g^1\rangle), \tag{103}$$

$$|U'_\mu 3/2\rangle=\frac{1}{\sqrt{2}}(-|-1/2\rangle|e_g^2\rangle+|3/2\rangle|e_g^1\rangle), \tag{104}$$

$$|U'_\nu 3/2\rangle=\frac{1}{\sqrt{2}}(|-3/2\rangle|e_g^2\rangle+|1/2\rangle|e_g^1\rangle) \tag{105}$$

and $E(J_A)$ is given by Eq. (54). Since, the operator $2S_Z+L_Z$ has matrix element only between the states $\Delta J_A=0$ and $\Delta J_A=\pm 1$, only the states of $J_A=3/2$ are connected to $J_A=1/2$. Moreover, only S_Z term has matrix element between the states of $|U'_k 3/2\rangle$ and $|U'_k 1/2\rangle$. Therefore, the first order correction becomes as follows,

$$\Delta^{(1)}(W/\mu_B H)_k$$
$$=\frac{(C_2/t_2)\langle J_A=\tfrac{1}{2},-\tfrac{1}{2}|S_z|\tfrac{3}{2},-\tfrac{1}{2}\rangle\langle\tfrac{3}{2},-\tfrac{1}{2}|T_0^{(2)}|\tfrac{1}{2},-\tfrac{1}{2}\rangle\langle e_g^1|U_0^{(2)}|e_g^1\rangle}{E(\tfrac{3}{2})-E(\tfrac{1}{2})}, \tag{106}$$

in which t_2 is given in Table IV and the matrix element of S_z is given by the following expression,

$$\langle(7/2,3)1/2,-1/2|S_z|(7/2,3)3/2,-1/2\rangle$$
$$=\frac{-1}{2}\sqrt{\frac{[(7/2+3+1)^2-(3/2)^2][(3/2)^2-(7/2-3)^2]}{3/2}}$$
$$\cdot\frac{(-)^2}{\sqrt{2}}\left\langle 3/2,1,-\frac{1}{2},0\middle|1/2,-\frac{1}{2}\right\rangle=\sqrt{3}. \tag{107}$$

The matrix elements of $T_0^{(2)}$ is given using Eq. (78) as follows,

$$\langle(1/2,3)7/2,3;\ 3/2,-1/2|\ T_0^{(2)}|\ (1/2,3)7/2,3;\ 1/2,-1/2\rangle$$
$$=\frac{1}{\sqrt{5}}(-)^{3/2+1/2+7/2+2+3+1/2}\sqrt{4\cdot2}\begin{Bmatrix}3 & 2 & 3\\ 1/2 & 7/2 & 3/2\end{Bmatrix}\langle 3/2,1/2,-1/2,1/2|2,0\rangle$$
$$=-\sqrt{1/4\cdot35}\,. \tag{108}$$

The final factor is given in Eq. (81) as $\sqrt{2/35}$. Therefore,

$$\Delta^{(1)}(W/\mu_BH)_k=\frac{C_2\cdot\sqrt{3}\cdot\sqrt{8\cdot3\cdot5^2\cdot7^2}\cdot\sqrt{1/4\cdot35}\cdot\sqrt{2/35}}{\Delta_F\cdot9/7}$$
$$=\frac{-14}{3}\frac{C_2}{\Delta_F}\,. \tag{109}$$

Moreover the following relations are easily obtained.

$$\Delta^{(1)}(W/\mu_BH)_\mu=\Delta^{(1)}(W/\mu_BH)_k=-\Delta^{(1)}(W/\mu_BH)_{\lambda,\nu}, \tag{110}$$

and then the first order correction to the ξ's parameters are given by

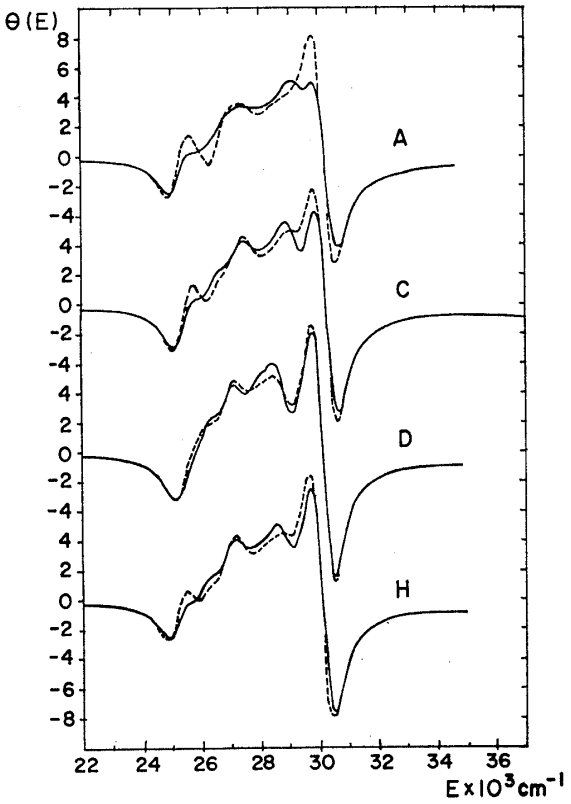

Fig. 9. Faraday rotation spectrum for the e_g band. The full lines correspond to the limit of the small magnetic polarization and the dashed lines correspond to the limit of the saturation of the magnetic polarization.

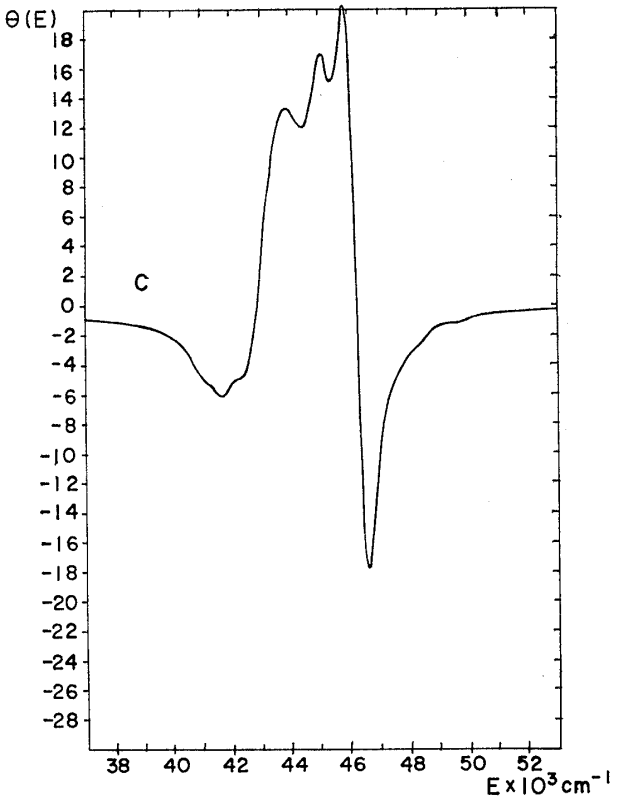

Fig. 10. Faraday rotation spectrum for the t_{2g} band.

$$\Delta\xi_1^{(1)} = -\frac{28}{3}\frac{C_2}{A_F} \quad (111)$$

and

$$\Delta\xi_2^{(1)} = 0. \quad (112)$$

Using the values of A_F and the experimental value of ξ_1, the value for C_2 is determined approximately to be -18cm^{-1}. This value is in good agreement with the value determined from the absorption curve. In the second order perturbation, the value of ξ_2 is reduced about 10% mainly due to the effect of S_2 term. This is also consistent with the experimental results.

The Faraday rotation spectra are shown in Figs. 9 and 10, in which the same values as in Fig. 5 are used for the various parameters. In these figures, the values for the following expression are given.

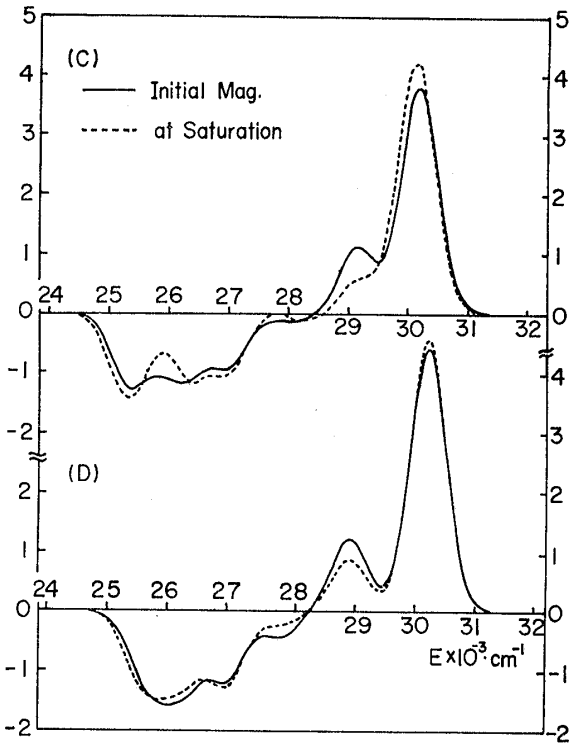

Fig. 11. Circular dichroism spectra for the e_g band. The full lines correspond to the limit of the small magnetic polarization and the dashed lines correspond to the limit of the saturation of the magnetic polarization.

$$F(E) = (\langle S_z\rangle/S)^{-1}\Theta(E). \quad (113)$$

In Fig. 11, the spectra for the circular dichroism $D_c(E)$ are shown

$$D_c(E) = (\langle S_z\rangle/S)^{-1}E(f_+(E) - f_-(E)). \quad (114)$$

In the above two equations,

$$\langle S_z\rangle = \frac{\sum S_z e^{-\mu_B H S_z/\kappa T}}{\sum e^{-\mu_B H S_z/\kappa T}} \quad (115)$$

in which H is the effective magnetic field, μ_B the Bohr magneton, T the absolute temperature and κ the Boltzmann constant.

In Figs. 9, 10 and 11, both of the values for the saturation magnetization and for the limit of the small magnetization are given. From the difference of the two values, the field dependence of the Faraday rotation or the circular dichroism can be deduced as shown in the following example. At 29000cm^{-1} of Fig. 11 (C), the full line has a larger value than the dashed line. This indicates that the circular dichroism, at this wave number in this

case, saturates more rapidly than the magnetization. On the other hand, at 30200cm^{-1} in Fig. 11 (C), the circular dichroism has slower saturation than the magnetization.

The spectra themselves for the Faraday rotation and the circular dichroism look rather insensitive to the values of the anisotropic parts of the Coulomb and exchange interaction. However, the field dependences of them are rather sensitive to the Coulomb and the exchange parameters. Unfortunately, we have not now precise experimental data on this point.

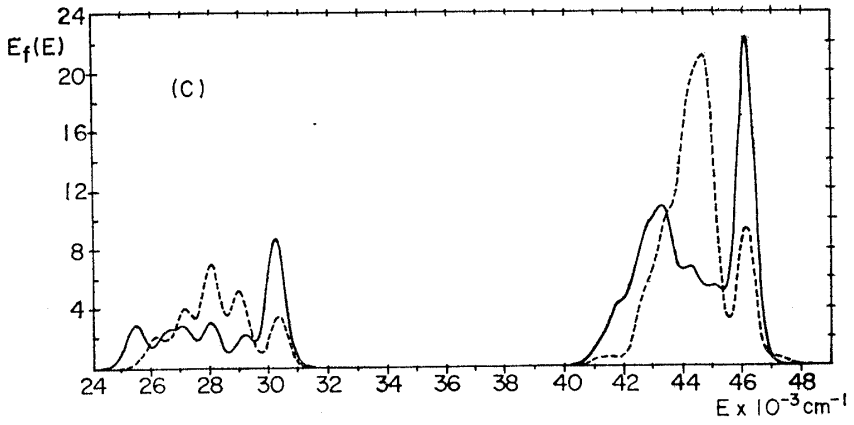

Fig. 12. The spectrum for the linear dichroism are shown, in which the full line shows absorption curve for the perpendicular polarization of the light and the dashed line shows that for the parallel polarization. Moreover, the ground state $4f^7(^8S_{7/2})$ is assumed to be fully polarized.

In Fig. 12, the linear dichroism is shown. Note that in these spectra, the peaks become clearer than those for the unpolarized light. Therefore the experiment on the polarized light would give more precise information on the excited state for the transitions of $4f^7 \rightarrow 4f^6 5d$.

Finally, the coupling scheme which describe the state in the configuration of $4f^6(^7F)5d$ in the CaF_2 type crystals is given as follows. At first, the crystal field on the $5d$-electron divides the $5d$ states into two groups, t_{2g} and e_g. In the second, the isotropic part of the exchange interaction between the $5d$ and $4f$ electrons gives the exchange splitting into the states of the total spin $S=7/2$ and $S=5/2$. Among the remaining interactions, the anisotropic parts of the Coulomb and the exchange interactions and the spin-orbit interaction for the $4f$ electron has the largest effects. Especially for the states of e_g with $S=7/2$, the quantum number for the composite angular momentum J_A, which is given by

$$\begin{aligned} \boldsymbol{S} &= \boldsymbol{S}_d + \boldsymbol{S}_F, \\ \boldsymbol{J}_A &= \boldsymbol{S} + \boldsymbol{L}_F, \end{aligned} \tag{116}$$

can be a good quantum number approximately. For the states with large

values of J_A, the energy differences between the states with the neighbouring values of J_A are large enough to give the systematic peaks in the absorption curve. However, for the states of e_g, $S=5/2$, the effects of the anisotropic parts of the Coulomb and the exchange interaction are so large that the spectrum of this part is expected to have no systematic structure.

In the state of t_{2g}, the spin-orbit interaction for the $5d$-electron have the matrix elements and have the effects as shown in Eq. (57) and in Fig. 3. In this case, therefore, the anisotropic parts of the Coulomb and the exchange interaction can easily mix together at least the states with neighbouring values of J_A and the spectrum have no systematic structure. However, the total width of the t_{2g} band is mainly given by the spin-orbit interaction in a $4f$-electron. This character might be observed in the magnetic dichroism of this band.

References

1) A. A. Kaplyanskii and P. P. Feofilov, Opt. Spectry **13** (1962), 129.
2) M. J. Freiser, S. Methfessel and F. Holtzberg, J. Appl. Phys. **39** (1968), 900.
3) P. Kisliuk, H. H. Tippins, C. A. Moore and S. A. Pollack, Phys. Rev. **171** (1968), 336.
4) Y. R. Shen, Phys. Rev. **134** (1964), A661.
Y. R. Shen and N. Bloembergen, Phys. Rev. **133** (1964), A515.
5) Y. R. Shen, Phys. Rev. **133** (1964), A511.
6) D. S. McClure, Adv. Solid State Phys. **9** (1959), 400.
7) W. R. Callaham, J. Opt. Soc. Am. **53** (1963), 695.
8) D. S. McClure and Z. Kiss, J. Chem. Phys. **39** (1963), 3251.
9) B. W. Bryant, J. Opt. Soc. Am. **55** (1965), 771.
10) B. G. Wybourne, *Spectroscopic Properties of Rare Earths* (John Wiley & Sons, Inc., 1965), p. 62.
11) See for example, A. Messiah, *Quantum Mechanics, Appendix C* (North-Holland Publishing Company, Amsterdam, 1964).
12) W. A. Crossley, R. W. Cooper and J. L. Page, Phys. Rev. **181** (1969), 896.